

Research on heliostat field design based on multi constraint particle swarm optimization algorithm

Ang Gao^{1,*}, Xiangru Yan², Jiayi Hu³

¹School of Electrical and Electronic Engineering, Shandong University of Technology, Shandong, Zibo, 255000, China

²School of Mathematics and Statistics, Shandong University of Technology, Shandong, Zibo, 255000, China

³School of Transportation and Vehicle Engineering, Shandong University of Technology, Shandong, Zibo, 255000, China

*Corresponding author: Y15563720713@163.com

Abstract: In the context of global new energy development and low-carbon economy, optoelectronics is expected to become the dominant energy source in China's future. Among them, tower solar thermal power generation technology that utilizes heliostat field light harvesting and photothermal conversion is the focus of development, but how to improve its power generation efficiency is urgent. Therefore, the paper studied how to reasonably configure the heliostat field, adjust the size, quantity, relative position, and parameters of the receiving tower, and fully utilize solar energy resources to maximize solar radiation energy. The paper propose a mirror field layout design based on multi constraint particle swarm optimization algorithm, and conduct specific research on its initial design, efficiency calculation, and layout optimization. The paper first established the three-dimensional coordinates of the heliostat based on formulas such as solar altitude angle, solar azimuth angle, and DNI, calculated the position and optical path tracking of the sun and heliostat to obtain the efficiency of the heliostat, and then calculated the thermal power output of the mirror field. The obtained results provide the basic data for the next step of analysis.

Keywords: Multivariate analysis, Three-dimensional coordinate system, Heliostat position

1. Introduction

Tower solar thermal power generation technology stands out rapidly among numerous solar power generation technologies due to its advantages such as high concentration ratio, high system efficiency, and good power quality, and has very broad development prospects [1]. However, due to the increase in mirror field capacity of photothermal power plants, the problem of low efficiency of existing mirror fields has become increasingly prominent. Through in-depth analysis of the mirror field design of tower solar thermal power plants, a systematic review and comparison of key algorithms such as initial layout, efficiency calculation, and layout optimization in different mirror field designs are conducted, providing ideas and theoretical references for the construction and mirror field design of tower solar thermal power plants. This plays an important role in efficiently collecting and utilizing solar energy and improving the economic benefits of power plants [2]. The geographical location of the heliostat field, namely longitude, latitude, and altitude, has been determined. The scope of the heliostat field is a circular area with a radius of 350m, and there must be a space within a radius of 100m around the heat absorption tower. Therefore, heliostats cannot be installed. Design and optimize the overall layout plan of the heliostat field while meeting the requirements of not touching the ground and corresponding maintenance during the fine adjustment process of the heliostat.

2. Determination of the position of the sun and positioning mirror

2.1 Establishment of Mirror Field Coordinate System

This article places the absorption tower at the center of the entire circular heliostat field, and the size and height of the heliostat have been determined. Provide data on the center position of the heliostat. To accurately represent the position of the heat absorption tower and heliostat, this article establishes the

mirror field coordinate system with the center of the circular mirror field area as the origin, the east direction as the positive axis, the north direction as the positive axis, and the zenith direction as the positive axis [3], as shown in Fig 1. Among them, point C is the center of the heliostat, and its coordinates are $(x_c, y_c, 0)$. The other physical quantities related to angle and orientation will be specifically solved in the following text.

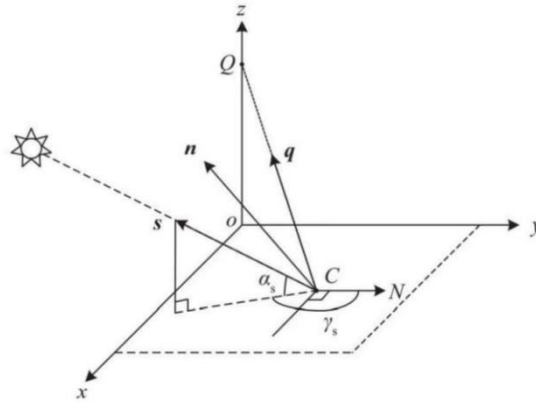


Figure 1: Model diagram of heliostat field coordinate system

Based on known data, draw a schematic diagram of mirror field arrangement in the mirror field coordinate system as shown in Fig 2 [4].

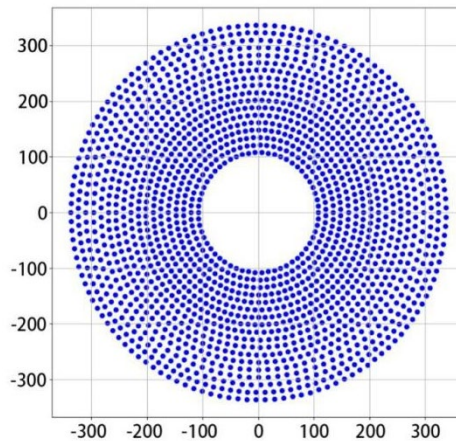


Figure 2: Spatial layout of heliostat field

Assuming that the arrangement of heliostats in the mirror field follows a radial uniform distribution, the distance between the center points of each heliostat and a 100m concentric ring can be calculated to verify the hypothesis.

2.2 Determination of the Sun's Position

Due to the continuous revolution and rotation of the Earth, the position of the sun will change over time relative to a certain heliostat, causing a change in the normal direct irradiance of the sun projected onto the heliostat field, which in turn affects the energy reflected by the heliostat onto the surface of the heat collector. This causes the adjustment of the azimuth and elevation angles of the heliostat itself to ensure that the reflected light smoothly falls into the absorption range of the heat collector. Therefore, the determination of the position of the sun at a certain time is the first issue that needs to be addressed in this article. The position of the sun can be represented by the sun's altitude angle [5] α_s and the sun's azimuth angle [6], γ_s both of which are calculated as follows:

$$\sin \alpha_s = \cos \delta \cos \varphi \cos \omega + \sin \delta \sin \varphi \quad (1)$$

$$\cos \gamma_s = \frac{\sin \delta - \sin \alpha_s \sin \varphi}{\cos \alpha_s \cos \varphi} \quad (2)$$

The calculations involving other parameters during the calculation process are as follows

ω ---- Suntime angle, δ ---- Solar declination angle

$$\omega = \frac{\pi}{12}(ST - 12) \quad (3)$$

$$\sin \delta = \sin \frac{2\pi D}{365} \sin \left(\frac{2\pi}{360} 23.45 \right) \quad (4)$$

φ ---- local latitude, ω ---- Suntime angle,

The above equation involves two date related parameters, where ST represents the local time and D represents the difference between the current day and the vernal equinox. Please note that the vernal equinox should be counted from day 0. Draw a three-dimensional map of the changes in solar altitude and azimuth during the day, as shown in Fig 3 and 4.

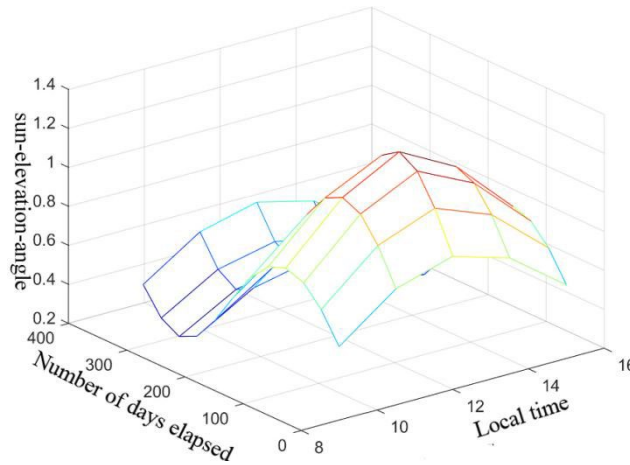


Figure 3: Schematic diagram of the variation of solar altitude angle over time

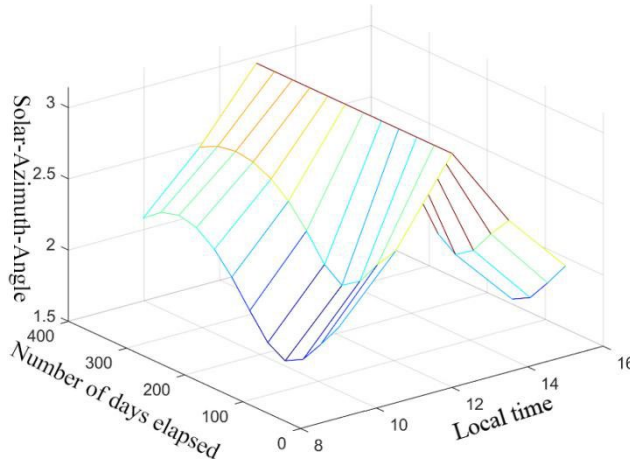


Figure 4: Schematic diagram of changes in solar azimuth angle over time

2.3. Determination of heliostat position

Based on the apparent motion law of the sun, the next step in this article is to calculate the position of the heliostat relative to the sun and the collector, which is the unit vector \vec{q} pointing towards the center of the collector and the unit vector \vec{s} pointing towards the direction of the sun at the center of

the heliostat.

$$\vec{q} = \left(\frac{-x_c}{\sqrt{x_c^2 + y_c^2 + z_q^2}}, \frac{-y_c}{\sqrt{x_c^2 + y_c^2 + z_q^2}}, \frac{-z_q}{\sqrt{x_c^2 + y_c^2 + z_q^2}} \right) \quad (5)$$

$$\vec{s} = (\cos \alpha_s \sin \gamma_s, \cos \alpha_s \cos \gamma_s, \sin \alpha_s) \quad (6)$$

According to the law of reflection, the azimuth angle γ_h and elevation angle α_h of the heliostat can be obtained by the following formula:

$$\tan \gamma_h = \frac{\cos \alpha_s \sin \gamma_s \sqrt{x_c^2 + y_c^2 + z_q^2} - x_c}{\cos \alpha_s \sin \gamma_s \sqrt{x_c^2 + y_c^2 + z_q^2} - y_c} \quad (7)$$

$$\sin \alpha_h = \frac{\sin \alpha_s \sqrt{x_c^2 + y_c^2 + z_q^2} - z_q}{\sqrt{x_c^2 + y_c^2 + z_q^2} \cdot |\vec{s} + \vec{q}|} \quad (8)$$

The position of the heliostat relative to the absorption tower is represented by the apparent height angle α_t of the absorption tower and the azimuth angle γ_t of the heliostat relative to the absorption tower. The calculation method is as follows:

$$\tan \alpha_t = \frac{\frac{-z_c}{\sqrt{x_c^2 + y_c^2 + z_q^2}}}{\sqrt{\left(\frac{-x_c}{\sqrt{x_c^2 + y_c^2 + z_q^2}} \right)^2 + \left(\frac{-y_c}{\sqrt{x_c^2 + y_c^2 + z_q^2}} \right)^2}} \quad (9)$$

$$\tan \gamma_t = \frac{\frac{-x_c}{\sqrt{x_c^2 + y_c^2 + z_q^2}}}{\frac{-y_c}{\sqrt{x_c^2 + y_c^2 + z_q^2}}} = \frac{x_c}{y_c} \quad (10)$$

At this point, the physical quantities related to the position of the sun and heliostat have been solved.

3. Establishment and Solution of an Optical Efficiency Model for Heliostats

This article calculates and outputs a series of indicators such as the annual average optical efficiency, annual average output thermal power, and annual average output thermal power per unit mirror area of the heliostat field. During the entire process of energy transmission, a series of factors such as incident light occlusion and atmospheric attenuation can cause energy loss and affect the optical efficiency of the heliostat. According to reference [7], the calculation process for the optical efficiency of a heliostat η is as follows:

$$\eta = \eta_{sb} \eta_{\cos} \eta_{at} \eta_{trunc} \eta_{ref} \quad (11)$$

The following will solve each physical quantity separately.

3.1 Cosine efficiency

Cosine loss is a phenomenon of reduced received energy caused by the direction of sunlight not always perpendicular to the heliostat surface, which affects the optical efficiency of the mirror field and

is reflected in cosine efficiency η_{\cos} . The calculation process is as follows:

$$\eta_{\cos} = \sqrt{\frac{\cos(2\theta) + 1}{2}} \quad (12)$$

Among them, θ is the incident angle of the heliostat, indicating that the angle between the unit vector \vec{q} pointing towards the direction of the collector and the unit vector \vec{s} pointing towards the direction of the sun is twice that of θ .

$$\cos(2\theta) = \frac{\vec{q} \cdot \vec{s}}{|\vec{q}| \cdot |\vec{s}|} = \vec{q} \cdot \vec{s} \quad (13)$$

By solving equations (12) and (13), the cosine efficiency η_{\cos} of the heliostat is obtained, and its distribution in the mirror field coordinate system is plotted. This article takes 9:00 am on March 21 as an example to display, as shown in Fig 5.

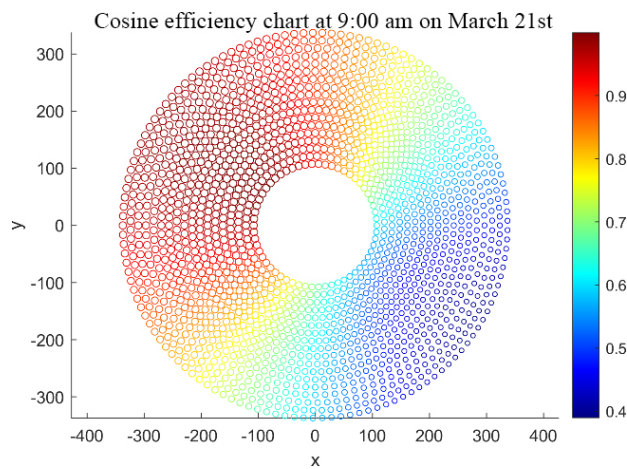


Figure 5: Distribution of cosine efficiency of heliostat field

3.2 Occlusion efficiency of incident light

In order to ensure that the output thermal power of the heliostat field meets the standard, under the limitations of the field size, there is inevitably obstruction between the heliostats, causing a certain loss of light intensity and affecting the optical efficiency of the heliostat. The calculation process of incident light occlusion efficiency [8] η_{sb} is as follows:

$$\eta_{sb} = \frac{d \tan \alpha_s}{\omega \cos \alpha_h (\tan \alpha_s + \tan \alpha_h)} \quad (14)$$

The factors that affect the occlusion efficiency of incident light η_{sb} include:

d ---Heliostat spacing, ω ---Heliostat width

Solve to obtain the incident light occlusion efficiency η_{sb} and draw its distribution map in the mirror field coordinate system. This article takes 9:00 am on March 21 as an example to display, as shown in Fig 6.

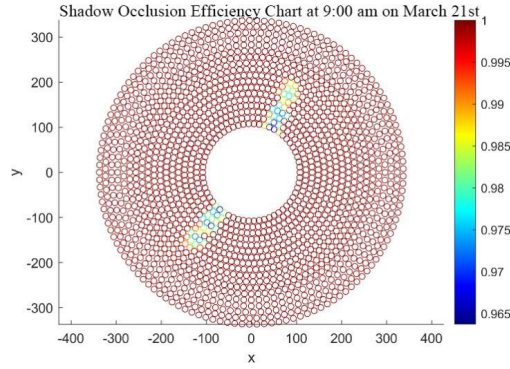


Figure 6: Distribution of Occlusion Efficiency of Incident Light in the Heliostat Field

3.3 Truncation efficiency

The truncation efficiency [9] reflects the phenomenon of the shift or overflow of the solar spot reflected by the mirror field when it falls into the receiving surface of the heat collector, that is, some sunlight fails to shine on the collector, causing the loss of the spot. For heliostats that are far away from the collector, the main reason is the diffusion of the solar spot, while closer heliostats are caused by the stretching of the spot caused by a larger reflection angle, i.e. the incident angle. The energy flow density distribution of the heliostat on the opening plane of the collector can be regarded as a Gaussian distribution, and the value of η_{trunc} can be obtained based on the calculation formula of truncation efficiency:

$$\eta_{trunc} = \frac{1}{2\pi\sigma^2} \iint e^{-\left(\frac{x^{*2}+y^{*2}}{2\sigma^2}\right)} dx^* dy^* \quad (15)$$

Where is σ solar half angle, with a value of:

$$\sigma = 2.325 \times 10^{-3} \text{ rad} \quad (16)$$

3.4 Atmospheric transmissivity

In the optical path, dust and particles in the air can cause attenuation of reflected light, so the atmospheric transmittance η_{at} is affected by the distance d_{HR} from the center of the mirror to the center of the collector [10]. The calculation formula is as follows.

$$\eta_{at} = 0.99321 - 0.0001176d_{HR} + 1.97 \times 10^{-8} \times d_{HR}^2 \quad (d_{HR} \leq 1000) \quad (17)$$

The mirror reflectance is η_{ref} , with a constant of 0.92. Through the above calculation process, the optical efficiency of a single-sided heliostat is finally output through formula (11), and the distribution map of heliostat optical efficiency η in the mirror field coordinate system is drawn. This article takes 9:00 am on March 21 as an example to display, as shown in Fig 7.

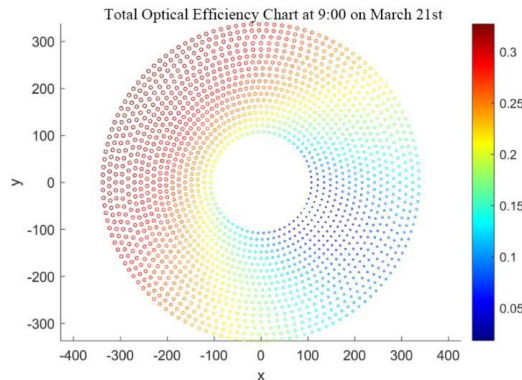


Figure 7: Distribution of optical efficiency of heliostats

3.5 Solution of Thermal Power Model for Heliostats

The output thermal power E_{field} of the heliostat field will be directly affected by the optical efficiency η of the heliostat, and its calculation process is as follows:

$$E_{field} = DNI \cdot \sum_i^N A_i \eta_i \quad (18)$$

DNI ---Normal direct radiation irradiance, N ---Total number of heliostats

A_i ---The lighting area of the i -side heliostat, η_i ---Optical efficiency of the i -side heliostat

Which involves the calculation of normal direct radiation irradiance DNI .

$$DNI = G_0 \left[a + b \exp\left(-\frac{c}{\sin \alpha_s}\right) \right] \quad (19)$$

$$\begin{cases} a = 0.4237 - 0.00821(6 - H)^2 \\ b = 0.5055 + 0.00595(6.5 - H)^2 \\ c = 0.2711 + 0.01858(2.5 - H)^2 \end{cases} \quad (20)$$

The formula involves the determination of two parameters, with the value of the solar constant G_0 being $1.366 \text{ KW} / \text{m}^2$ and the altitude of H . Based on the location information in the question, it can be determined that the value is 3. Through this process, DNI was calculated, and the reason for the length is only to display the local DNI value at 9:00 am on the 21st of each month for 12 months of a year, as shown in the table. A three-dimensional map of DNI changes in different months and a day was drawn, as shown in Fig 8.

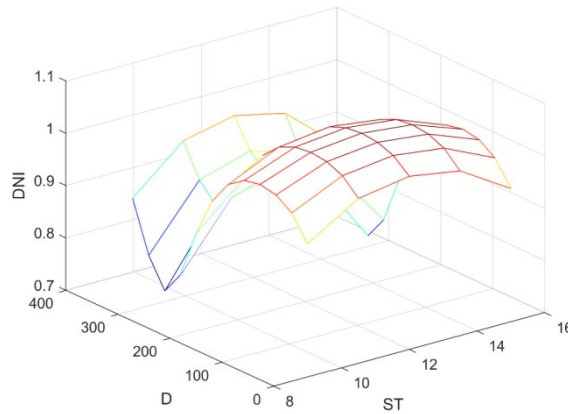


Figure 8: Schematic diagram of DNI changing over time

Bring in formula (20) and solve for the value of the output thermal power E_{field} of the heliostat field. For the average output thermal power E_u per unit area of the mirror, there is:

$$E_u = \frac{E_{field}}{\sum_i A_i} \quad (21)$$

Based on the above solving process, the calculated values of physical quantities related to daily optical efficiency and thermal power are finally output by month, and the average is calculated by adding each month to output the corresponding annual average index, and the results are obtained.

4. Conclusions

According to the calculation results, the annual average optical efficiency of the heliostat field is 0.45, which means that 45% of the heliostat can reflect solar energy onto the collector normally throughout the year. The annual average cosine efficiency is 0.76, indicating that the heliostat can correctly focus sunlight onto the center of the collector at different time points based on changes in the sun's position. The annual average shadow occlusion efficiency is 0.91, which means that the proportion of heliostats obstructed and unable to fully reflect sunlight during the year is only 9%. The annual average truncation efficiency is 0.75, indicating that the proportion of heliostats unable to capture the solar cone due to shape and installation height limitations is 25%. According to calculations, the annual average output thermal power of the heliostat field is 27.57 megawatts (MW), indicating that the system can stably convert solar energy into thermal energy. Finally, the average annual thermal power output per unit area of a mirror is 0.44 kilowatts per square meter (kW/m²), indicating that a heliostat mirror can generate 0.44 kilowatts of thermal energy per square meter. In summary, the heliostat field performs well in terms of optical efficiency and thermal energy conversion ability, providing a reliable technical foundation for the construction of new energy power systems.

References

- [1] Yang Hongtao. *Research on the Focusing Model and Optimal Scheduling System of a Heliostat* [D]. Xi'an University of Technology, 2023
- [2] Qin Hua. *General layout and optimization of the power generation area of tower solar thermal power plants* [J]. *Electric Power Survey and Design*, 2023, (09): 66-72+78
- [3] Liu A, Fan S. *The Research on the Matching Design of the Ship-Engine-Propeller Based on Multi-Objective Particle Swarm Optimization*[C]//*International Workshop on Intelligent Systems & Applications*. IEEE, 2010.DOI:10.1109/IWISA.2010.5473726.
- [4] Fang Miaosen, Lu Jing, Jiang Yiwen. *Modeling of energy transfer efficiency and design of mirror field layout for heliostats* [J]. *Journal of Solar Energy*, 2021,42 (01): 112-116.
- [5] Qin Yang. *Research on Missile Based Integrated Navigation Technology Based on INS/GPS/Geomagnetism/Sun Azimuth* [D]. Nanjing University of Technology, 2020.
- [6] Gong Jianqiang. *Preliminary Exploration of Integrating the LAUNCH Cycle Concept into High School Geography Practice Activities - Taking the Production of a Sun Altitude Angle Measuring Instrument as an Example* [J]. *Geography Teaching*, 2023 (18): 32-35
- [7] Liu Jiaojiao. *Simulation Modeling of Photovoltaic Power Generation Systems and Efficiency Analysis of Photovoltaic Blocking Power Generation* [J]. *Rural Electrification*, 2022 (11): 61-64+68
- [8] Zhang Ping, Xi Zhengwen, Hua Wenhan, Wang Juanjuan, Sun Dengke. *Calculation method for optical efficiency of solar tower photothermal mirror field* [J]. *Technology and Market*, 2021,28 (06): 5-8
- [9] Hu Liang, Zhang Ping, Xi Zhengwen, et al. *Ray tracing and artificial neural network calculation method for truncation efficiency of tower photothermal power generation focusing field* [J]. *Dongfang Electric Review*, 2020,34 (03): 64 69+75.
- [10] Liu Zonghao, Mao Yuxin, Qu Xiaojun, etc *Estimation of Laser Detection Distance Based on Atmospheric Transmittance* [C]//*The System Simulation Professional Committee of the Chinese Society of Automation and the Simulation Technology Application Professional Committee of the Chinese Society of Simulation. Proceedings of the 23rd China System Simulation Technology and Application Academic Annual Conference (CCSSTA23rd 2022)*. Hefei University of Technology Press, 2022:5.